ABSTRACT

Title of thesis: A MODEL TO PREDICT THE SIZE OF
3D REGOLITH CLUMPS ON PLANETARY BODIES

Anand Patel
Master of Science, 2020

Thesis directed by: Professor Christine Hartzell
Department of Aerospace Engineering

Prior investigations of the behavior of regolith on the surface of planetary bodies has considered the motion and interactions of individual grains. Recent work has shown the significance of cohesion in understanding the behavior of planetary regolith, especially on small, airless bodies. Surficial regolith grains may detach from a planetary body due to a variety of phenomena, including aeolian effects, spacecraft operations, micrometeoroid bombardment and electrostatic lofting. It is well known in terrestrial powder handling that cohesive powders tend to form clumps. We present an analytical theory for the size of regolith clumps that are likely to form and be easier to detach from a surface than their constituent grains, assuming monodisperse, spherical grains. The model predictions are significant for our interpretation of the surface of asteroids, as well as understanding a variety of phenomena on planetary bodies and designing of sampling spacecraft.

A MODEL TO PREDICT THE SIZE OF
3D REGOLITH CLUMPS ON PLANETARY BODIES

by

Anand Patel

Thesis submitted to the Faculty of the Graduate School of the
University of Maryland, College Park in partial fulfillment
of the requirements for the degree of
Master of Science
2020

Advisory Committee:
Professor Christine Hartzell, Chair/Advisor
Professor David Akin
Professor Ray Sedwick

Acknowledgments

I owe my gratitude to my research advisor Dr. Christine Hartzell for her guidance and support throughout my graduate experience, to my lab mates who were always reliable for positivity and optimism, and my family for their continuing support and belief in me.

Table of Contents

List of Figures

Chapter 1:   Introduction

1.1   Cohesion's Effect on Regolith

A regolith grain on the surface of a planetary body can be acted upon by gravity, cohesion, air drag and an electrostatic force (the product of the grain's charge and local electric field strength). Grains can detach from the surface of a planetary body through a variety of mechanisms, such as micrometeoroid bombardment, saltation, spacecraft operations, and electrostatic lofting.

Cohesion dominates the behavior of sub-cm regolith on small airless bodies [1]. Scheeres et al. [1] establish asteroids as being composed of granular structures, agglomerates of regolith grains, through a survey of asteroid spin rates and observational evidence of porosity in bodies like Eros and Itokawa. The rapid rotation of asteroids supports the presence of a strong cohesive force since its absence would lead to the body losing mass through material ejection, and the survey presented highlights work showing that even small degrees of cohesion play a large role in stabilizing small bodies. This led to the "rubble pile model for asteroid morphologies", or the notion that larger asteroids are aggregates of smaller particles. Scheeres et al.'s [1] second point is that high density regions on asteroids resting upon each other, with open voids in between, would hypothetically still yield large macro-

porosities across the asteroid, supporting the rubble pile theory. Our proposed clumping model is consistent with the asteroid granular mechanics formulated by Scheeres et al. [1]. This work identifies van der Waals cohesion as a significant physical force in the asteroid environment, capable of competing with weight and even exceeding forces caused by electrostatics and solar radiation pressure. Scheeres et al. [1] interpret terrestrial experiments dealing with cohesive power, with their cohesion model, and proposes the idea of asteroids being composed of relatively fine grains, or agglomerates of these grains, bound together by van der Waals cohesion. Two relevant applications of these findings, highlighted in Scheeres et al. [1], are the proposal that the dominant cm-sized grains in Itokawa's Muses Sea region might be clumps of smaller particles held together by cohesion and that cohesion can play a role in dust lofting and migration on the surface of asteroids. The results from this work motivate terrestrial experiments with cohesive powder to model the asteroid environment.

Examples of such experiments are present in research into electrostatic lofting of individual grains, which revealed the preferential lofting of intermediately sized grains [2, 3]. Hartzell and Scheeres [2] establish an expression for the cohesion between two spherical particles of equal size, as a function of grain size, Hamakar constant, and a cleanliness factor corresponding to the thickness of absorbed molecules between grains. Our work modifies this expression for cohesion on a grain through substituting the reduced Hamakar constant for lunar regolith and coordination number, the number of contacts between particles, for the Hamakar constant and cleanliness factor respectively. As a result, we relate cohesion between

spherical grains to the number of contacts. Hartzell and Scheeres [2] also demonstrate that cohesive forces dominantly influence the electrostatic force required to detach small grains ($\leq$ 1 mm, Moon), whereas gravity dominantly influences magnitude of force required to detach large grains. As a result, this work implies that grains electrostatically lofted from asteroids would be larger than those around the moon since gravity is significantly less. Since cohesion is stronger between small grains in powder than larger grains, the preferential motion of larger grains might be enabled [2]. This idea is supported by Hartzell and Scheeres [2] showing that variations in cohesive strength impact the electrostatic force required to detach grains more than variations in gravity or seismic shaking. Hartzell et al. [3] experimentally show the preferential detachment of intermediate-sized grains over small and large grains. The experimental set up used uniformly sized polystyrene microspheres as regolith grain simulant, on a negatively biased plate with an argon plasma sheath above. The electric fields created point upwards and away from the center of the grain pile, so detachment of grains (once overcoming cohesion and gravity) means separation from the pile and redeposition away from the pile's center. These experiments showed that 15 micron grains require a weaker electric field to detach from a pile than 5 micron or 25 micron grains [3]. Somewhere in between grains that weigh too much due to size and very small, light grains that experience too much cohesion exists an intermediate grain easier to detach that either of the previous. Our work shows that this intermediately-sized grain can be replaced by some detachable clump that experiences less cohesion than its constituent small grains.

The cohesion between a clump and grains is characterized and shown to be less

3

than cohesion just between grains in Sánchez and Scheeres [4]. This work considers a spherical "boulder" resting partially in or upon a bed of loose grains. Consistent with rubble pile theory, these boulders, composed of grains with high density packing, are adhered to the larger body by van der Waals cohesion imparted by the looser grains surrounding them. The macro-porosity of this system corresponds to the high porosity asteroids characterized as rubble piles [4]. The more that these boulders are covered by loose grains, the stronger they are adhered to the larger bulk. The strength of the van der Waals cohesion acting on the boulder is dependent on the number of contacts [4] between the grains on the boulder's surface and the surrounding bulk grains imparting cohesion. Sánchez and Scheeres [4] describe this number of contacts in terms of the mean coordination number (the average number of neighboring particles that touch a given grain). Intuitively speaking, the number of contacts is reduced for a boulder since each grain along its surface only faces the bulk grains from the outward side normal to the surface. This gives fewer opportunities for contact, and van der Waals forces, than for a grain in bulk surrounded by other grains on all sides. Sánchez and Scheeres [4] model this by reducing the coordination number. Therefore, we expect the cohesion on a boulder to be less than the cohesion on a grain, for reasonable boulder sizes that are not many orders of magnitude larger than their constituent grains. The expression given by Sánchez and Scheeres [4] for cohesion on a boulder is a function of the reduced Hamakar constant (like our modified expression from Hartzell and Scheeres [2]), boulder cross-sectional area, local grain packing fraction inside the boulder, mean coordination number, and grain size. We use this expression to determine cohesion

on a clump.

1.2   Observations of Regolith Clumps

Terrestrially, it is observed (in a variety of fields dealing with cohesive powders) that clumps of small grains are easier to detach than individual small grains [5]. Close-up observations of the lunar regolith from the Apollo era have previously been described as 'clumpy' [6]. Additionally, the detachment of regolith clumps has previously been hypothesized by Marshall et al. [5] and shown to occur in terrestrial experiments [5,7,8].

However, there is currently no model to predict when clumps will detach from the surface of a planetary body rather than individual grains, or the size of those clumps. The possible formation and preferential detachment of clumps of grains has significant implications for our understanding of various planetary processes and the design of spacecraft to interact with planetary surfaces.

1.2.1   Experimental Methods

Clumps of JSC-1 regolith simulant have been shown to form and preferentially loft over smaller fine grains through multiple methods of detachment [5]. In the experiments conducted by Marshall et al. [5], powders were subjected to three types of stress in order to incite detachment of grains; triboelectric charging (motivated by such effects on the Moon), monopolar charging through an electric field (motivated by plasma charging), and aerodynamic shear forces. For all three methods,

large clumps of grains, or sometimes large grains, were easily detached before any smaller grains. Marshall et al. [5] conclude that cohesive powder under electric fields (charged) or under aerodynamic stress fracture into aggregates more easily than into individual grains [5]. Fractures or defects form in the packing, from which preferential detachment of clumps is shown to occur. These experiments predict clumps to be easier to detach than individual grains in space-analog environments, but Marshall et al. [5] advocate for the development of an analytical approach to finding the size of aggregates released from a cohesive powder as a function of parameters such as cohesive strength, grain size, compaction, etc.

Terrestrial experiments from Durda et al. [7,8] study the size of clumps formed through avalanching of cohesive flour under a vacuum. These experiments used a sieve to pile flour grains onto the test bed, tilted the test bed until slope failure occurred, and surveyed the fallen powder for clump sizes. The ordinary un-bleached white flour grains had adsorbed water baked off using thermo-vacuum. The clumps formed ranged in size from over 0.5 mm in diameter to less than 10 mm in diameter, with significantly more clumps being on the smaller side of this range [8]. This work gives terrestrial clump size for cohesive powders formed experimentally under vacuum. However, this work does not establish a quantitative relationship between clump size and grain size, packing, or cohesion. As we see in Marshall et al. [5], there exist multiple methods for clump detachment and many methods involve a vertical component of ejection or motion. Slope failure is only one mechanism for clump formation, and it entirely involves lateral movement. These experiments demonstrate the need for an analytical model for describing the size of detachable

clumps.

1.2.2 Terrestrial Applications

A model that predicts the size of clumps and when they occur would improve our understanding of terrestrial clump movement across many industries. In the pharmaceutical industry, Dry Powder Inhalers (DPIs) use clumps of inert carrier particles and active, pharmaceutical particles as a drug delivery method [9]. Thus, variation in clump size as a function of the characteristics of the constituent particles is significant in controlling dosage. Coal dust can pose a hazard to workers through both inhalation and explosion risks [10]. An improved understanding of the size of clumps of coal dust would inform efforts to mitigate these hazards. Even printer toner particle size can influence the indoor air contamination of a space housing one or more printers [11], so being able to size clumps of toner particles could improve accuracy in assessing these risks.

1.2.3 Space Applications

It is known that larger grains than on Earth are capable of being suspended on Mars [12,13]. If clumps of particles are easier to detach from the surface of Mars through aeolian processes than individual grains, then the observations of large, suspended grains on Mars could be clumps. Our model for preferential clump detachment could also explain why the observed densities of dust in Martian wind are greater than predicted amounts based on models for dust detachment as a function

of wind speed [13, 14]. Additionally, the presence and motion of clumps can impact interpretation of "remote-sensing observations, affect sampling strategies, and have detrimental effects on manned and unmanned spacecraft on the surface" [13]. Similarly, the motion of regolith particles on airless bodies could have significant interaction with spacecraft operations.

1.3   Our Research Contribution

Considering the gravitational and cohesive forces acting on regolith grains, we present a model to predict the size of regolith clumps that are easier to detach than their constituent grains, as a function of grain size, packing fraction and central body size. We assume that all forces are collinear and act perpendicular to the surface. Additionally, we will predict the size of clumps likely to be present in situ by modeling the bulk regolith porosity as the result of less porous clumps separated by voids. We will primarily consider airless planetary bodies, but the results presented are also applicable to planets with atmospheres (e.g., the Earth and Mars). We presented our model at the 2019 Lunar Planetary Science Conference [15], and the main contributions of this thesis were accepted into the 2020 Lunar Planetary Science Conference under the title "Predicting 3D Cohesive Regolith Clump Size on Airless Bodies". The main contributions of this thesis have been submitted to the Journal of Geophysical Research: Planets under the title "A Model to Predict the Size of Regolith Clumps on Planetary Bodies".

1.4 Outline of Thesis

In Chap. 2, we present a survey of significant forces keeping regolith grains adhered to the surface of airless bodies. These forces constitute a force balance that can be solved for the largest clump constrained by the net downward force. Such clumps will be easier to detach from the surface of airless bodies than their constituent grains from bulk packing. We also derive an expression for the maximum number of grains in a clump, based on this force constrained clump size.

In Chap. 3, we present our geometric model for constraining clump size. This model governs which clumps will actually form *in situ*. We show how clump volume under this model depends on the relationship between bulk and local packing of grains. We consider the impact of intermediate parameters on geometrically constrained clump size.

In Chap. 4, we combine the geometric constraint on clump size with our force constraint on clump size. As a result, we determine the size of clumps easier to detach than their constituent grains *and* capable of forming for given planetary body, bulk packing fraction, and set of grain sizes. We present the predicted clump size for cm and mm sized grains on Bennu and the predicted grains per clump for cm sized grains on Bennu. We also show how changing our assumptions of cohesion between grains and cohesion between a clump and grains impacts our predicted clump size. We present observations on the relationship between maximum clump size and various parameters. Lastly, we show predicted clump sizes for 10s of micron sized grains on Earth and how these results match up to terrestrial experiments.

Chapter 5 provides the conclusion to the thesis.

Chapter 2:   Force Model for Constraining Clump Size

2.1   Overview

The net force adhering a regolith grain to a surface is the sum of the gravitational force and the cohesive force acting on the grain. In order to detach a grain from the surface, the net force away from the surface ('upwards') must be greater than the net force towards the surface ('downwards'). The net downward force varies with the size of the regolith grain. For small, fast rotating bodies, centrifugal and gravitational accelerations can be the same order of magnitude and the centrifugal force pulling grains upwards should be subtracted from the gravitational force, lessening the net downward force on grains. In order for a clump to detach rather than an individual grain, the net downward force on an individual grain must be greater than the net downward force on a clump of grains. This section derives an expression for maximum clump size that satisfies this condition (i.e., the largest clump that requires less force to detach than an individual grain).

2.2 Forces Acting on a Clump

We derive an expression for the forces acting on a clump of grains. Regolith grains are approximated as monodisperse spheres of uniform density. We assume that grains in a clump have a local packing fraction ϕ. The maximum value of ϕ is 0.74, corresponding to face-centered cubic and hexagonal close packing, and the minimum value is ϕ_b, where ϕ_b is the bulk packing fraction of the regolith. Figure 2.1 shows a sketch of the forces acting on a clump and grain in our model. Assuming a clump consists of grains packed into a 3-dimensional volume of height h, the equation for cohesion on a clump is [4]:

$$F_{c,clump} = \frac{A_h A_b \phi C_{avg}}{8R} \tag{2.1}$$

where R is the radius of the grains, A_b is the clump cross-sectional area, C_{avg} is the mean coordination number (the average number of contacts between a clump and its neighbors), and A_h is the reduced Hamaker constant for the regolith. The reduced Hamaker constant for lunar regolith is 0.036 N m^{-1} [4], which assumes a Hamaker constant of 5.14×10^{-20} J and a separation between grains due to adsorbed molecules of 1.17×10^{-10} m (about the diameter of an oxygen ion). C_{avg} is taken to be 4.5 [4]. Sánchez and Scheeres [4] note that C_{avg} will decrease with realistic (non-crystalline) granular packings. The sensitivity of our results to C_{avg} will be discussed in Section 4.3. An alternate method to characterize cohesion involves modeling the capillary force and quantifying the strength of this force through its relation to the change

in surface energy during particle contact formation [16]. However, we follow the implementations of the van der Waals force used in prior simulations of regolith particles [1, 2, 4].
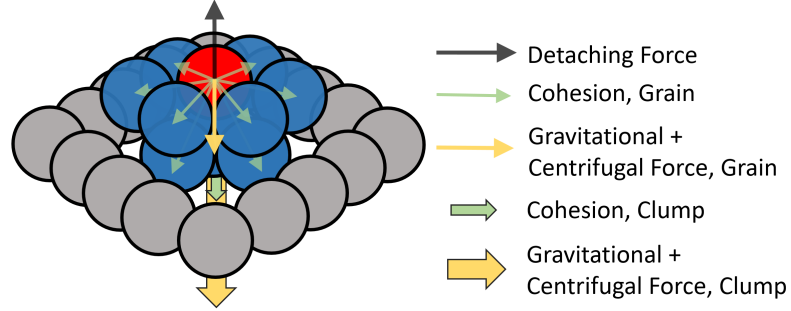
Figure 2.1: An idealized diagram showing the cohesion, gravitational, and centrifugal forces acting on a clump (red and blue grains) and grain (red grain) that oppose some force acting to detach from the surface, all within a rotating body frame. The bulk powder is denoted by grey grains and there exist gaps between the clump and bulk powder that signify void space in packing. When considering the detachment of a single grain, blue denotes neighboring grains, each exerting cohesive force, on the red grain being detached.

The gravitational force acting on a clump (Eqn 2.2) is derived for a known grain radius R and surface gravity g. The density of a regolith grain ρ is assumed to be 3200 kg m^{-3} [4]. The clump's volume V_{clump} is calculated by assuming the clump has a height h.

$$F_{g,clump} = V_{clump}\phi\rho g = A_b h \phi \rho g \tag{2.2}$$

2.3 Forces Acting on a Grain

The cohesive force on a single grain is described by [2]:

$$F_{c,grain} = A_h R C_{FCC} \tag{2.3}$$

where C_{FCC} is the mean coordination number for face-centered cubic (FCC) packing ($C_{FCC} = 12$). Crystalline packings of spherical 'grains' (or molecules) are commonly studied in materials science, and the maximum possible coordination number of a crystalline packing is 12 [17]. Cohesion is maximized when the coordination number is maximized (i.e., when a grain has the theoretical maximum of 12 contacts). An individual grain that would be detached from a regolith surface would have fewer than 12 contacts, since there will be no crystalline matrix on the 'top side' of the grain. The number of contacts on an individual regolith grain strongly depends on the packing of the surface. If the regolith surface has a fractal structure, a single regolith grain could have as few as 1 contact. For simplicity, we assume that $C_{FCC} = 12$. The effect of assuming a reduced coordination number is discussed in Section 4.3. Additionally, we note that $C_{FCC} \neq C_{avg}$. C_{FCC} considers the contacts to an individual grain from all directions, whereas C_{avg} considers the contacts to a clump that cross a single plane that must be severed for the clump to detach.

The gravitational force acting on an individual grain is:

$$F_{g,grain} = \frac{4}{3}\pi R^3 \rho g \tag{2.4}$$

14

2.4 Largest Clump Constrained by Net Downward Force

In order for a clump of grains to detach rather than a single grain, the net downward force on a single grain must exceed the net downward force on a clump. Thus, in order for a clump to be detached rather than an individual grain, the following expression must be satisfied:

$$F_{c,grain} + F_{g,grain} - F_{cent,grain} \geq F_{c,clump} + F_{g,clump} - F_{cent,clump} \tag{2.5}$$

$$F_{cent} = m r_s \omega^2$$

The centrifugal force F_{cent} is defined for clumps and grains based on their respective volumes, regolith density ρ, the body's radius at the surface r_s, and the body's spin rate ω. Substituting the expressions for the forces given by Eqn 2.1 through Eqn 2.4 into Eqn 2.5 and solving for the clump cross-sectional area (A_b) gives the maximum clump cross-sectional area ($A_{b,max}$) that is easier to detach than an individual grain:

$$A_h R C_{FCC} + \frac{4}{3}\pi R^3 \rho (g - r_s \omega^2) \geq \frac{A_h A_b \phi C_{avg}}{8R} + A_b h \phi \rho (g - r_s \omega^2)$$

$$A_{b,max} = \frac{8 A_h R^2 C_{FCC} + \frac{32}{3}\pi R^4 \rho (g - r_s \omega^2)}{A_h \phi C_{avg} + 8R\phi\rho h (g - r_s \omega^2)} \tag{2.6}$$

Eqn 2.6 gives the largest clump that is easier to detach than a single grain, as a function of grain radius R and local packing fraction ϕ. For small, fast rotating

bodies the centrifugal acceleration can be comparable to the gravitational acceleration. When gravitational and centrifugal accelerations are comparable (reducing the effective surface gravity), the role of cohesion in dictating clump size increases, resulting in larger clumps being easier to detach than individual grains.

Eqn 2.6 gives the maximum cross-sectional clump size that is easier to detach than an individual grain. Ideally, we would model clumps as cubic volumes with uniform side length given as a function of R, ϕ, and g. However, solving Eqn 2.6 for clump side length s does not yield an analytical solution. In Figure 2.2, we show that the cubic clump volume (black line) is bounded by clump volumes assuming height h as a function of grain radius R. We relate h to grain size through a, the discrete side length of a face-centered cubic or hexagonal close packed cube, where $a = 2\sqrt{2}R$. Figure 2.2 compares the volumes of clumps with heights of $2a, 3a$, and $4a$ to cubic clumps of 5 mm grains on Bennu (assuming a surface gravity of 8.60×10^{-5} m/s^2, 245 m mean radius, and 4.296 h rotation period [18]) for a variety of clump packing fractions. Clumps with heights $2a$ and $4a$ bound the volume of the cubic clump, and we find this relationship holds for other grain radii and surface gravities. The volume of a cubic clump approaches the volume of a clump where $h = 4a$ as local packing fraction decreases in Figure 2.2. Note that our model's assumption of spherical, mono-disperse grains requires $\phi_b < 0.74$, and the packing fraction observed on asteroids is much less than 0.74. Eqn 2.6 provides an upper limit on clump size. If it is possible to produce and detach clumps with height $4a$, then it must be possible to produce and detach cubic clumps, since $h = 4a$ is an upper bound on cubic clump volume. As a result, we will assume a clump height of
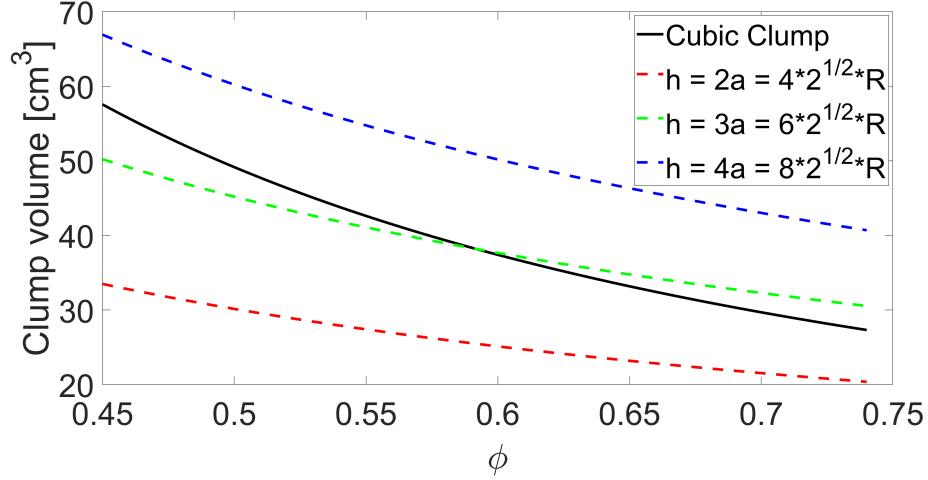
16

$4a$, or $8\sqrt{2}R$, moving forward.

Figure 2.2: Clump volume as a function of local packing fraction and assumed clump height h are compared for cubic clumps (black, uniform side length) and clumps with height $2a, 3a$ and $4a$. The plot is generated for 5 mm grains on Bennu (assuming Bennu's spin rate). Relations between the curves extend to other gravities and radii.

An expression for the maximum number of grains per clump as a function of surface gravity and grain size can be derived from the force constraint (Eqn 2.6) as follows:

$$V_{b,max} = A_{b,max}h\phi = A_{b,max}(8\sqrt{2}R)\phi \tag{2.7}$$

$$N_{grains,max} = \frac{V_{b,max}}{V_g} = \frac{A_{b,max}(8\sqrt{2}R\phi)}{\frac{4}{3}\pi R^3}$$

$$N_{grains,max} = \frac{48\sqrt{2}}{\pi} \frac{A_h C_{FCC} + \frac{4}{3}\pi R^2 \rho g}{A_h C_{avg} + 64\sqrt{2}R^2 \rho g} \tag{2.8}$$

Note that while Figure 2.2 shows a decreasing clump size as the local packing fraction increases, ϕ does not appear in Eqn 2.8. Thus, the decreasing clump size in Figure 2.2 is due to the tighter packing of the grains at higher local packing fractions, not necessarily a change in the number of grains in the clump.

Eqn 2.8 is plotted for several gravities and grain radii in Figure 2.3. We note that the centrifugal force is dropped in Eqn 2.8 because Figure 2.3 assumes no central body spin, since the spin rate can vary widely between bodies. For a given gravity and grain size, Figure 2.3 indicates the number of grains in the largest clump capable of being detached. Figure 2.3 shows that a clump composed of 57 2 cm radius grains can detach on Bennu, but only single 2 cm grains can detach under the substantially greater gravities of the Earth and Moon. Additionally, Figure 2.3 shows 57-grain clumps of 25 micron radius grains can detach on Earth.
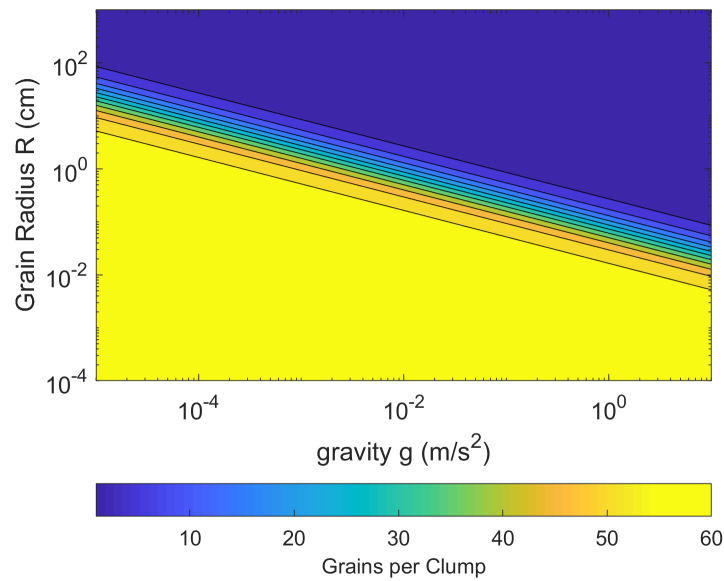

Figure 2.3: The maximum number of grains per clump as a function of gravity and grain size, assuming negligible centrifugal acceleration.

Chapter 3:   Geometric Model for Constraining Clump Size

3.1   Deriving the Geometrically Constrained Clump Size

In addition to the force constraint on the detachment of a clump, the bulk and local packing fractions place a geometric constraint on clump size. A given bulk packing fraction can be produced via clumps (with a higher local packing fraction) separated by defects. We define a defect to be a void in the packing lattice that serves as the structural weak point from which a clump can detach from the bulk powder.

Assume that a given bulk volume V has a known average porosity P. Porosity is related to the bulk packing fraction ϕ_b as follows:

$$\phi_b = 1 - P \tag{3.1}$$

Assuming N monodisperse spheres of radius R, the volume occupied by grains is $V_{g,tot}$:

$$V_{g,tot} = \frac{4}{3}\pi R^3 N$$

Porosity can be described by the fraction of empty space (V_e) in V:

$$P = \frac{V - V_{g,tot}}{V} = \frac{V_e}{V} \tag{3.2}$$

We assume that the total volume V, occupied by grains packed at bulk porosity P, is evenly discretized into uniform volumes of height q (see Figure 3.1). The cross section of these volumes is a triangle of height and base q. The volumes will be referred to as clumps, each containing grains packed with the local packing fraction ϕ (where $\phi \geq \phi_b$). Since the clumps can be more tightly packed than the bulk, empty regions (defects) of length g_{defect} form between these clumps. The volume of grains is given by Eqn 3.3 where V_q is the total volume of the clumps.

$$V_{g,tot} = \phi V_q \tag{3.3}$$

The void volume V_e is the summation of the defect volumes in V and the empty space in all the clumps. The total volume can be described by the sum of its empty and occupied space:

$$V = V_e + \phi V_q \tag{3.4}$$

Since the regolith grains are approximated by uniform spheres, the local packing fraction ϕ must be between ϕ_b and ϕ_{FCC}. The defects between ϕ-packed clumps must be less than $2R$ in length, since having a defect smaller than the diameter of a single grain eliminates the possibility of a grain falling into one of these spaces.

Combining Eqn 3.1, Eqn 3.2, and Eqn 3.4 yields the expression for V_q in terms
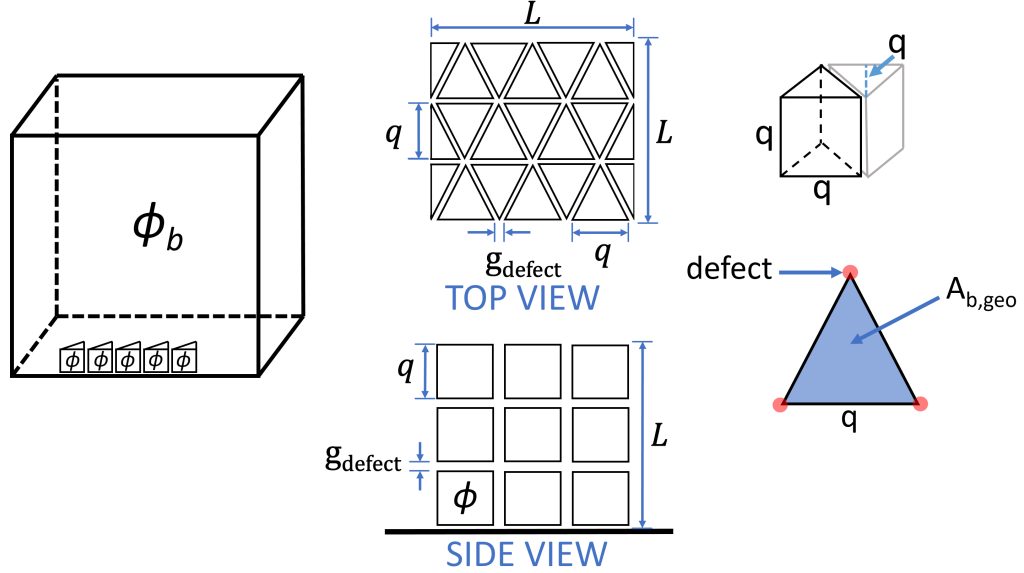
Figure 3.1: Diagram of the geometric model. The total volume V with bulk packing fraction ϕ_b contains clumps locally packed with packing fraction ϕ (where $\phi \geq \phi_b$) with a side length q. Clumps are separated by defects of length g_{defect}. Three defects are minimally required to form the cross-section of a clump $A_{b,geo}$.

of the known bulk packing fraction ϕ_b, total volume V, and local packing fraction ϕ.

$$V_q = \frac{V\phi_b}{\phi} \tag{3.5}$$

Along the total volume's side length L, there exist n clumps and n defects:

$$L = nq + ng_{defect} \tag{3.6}$$

where q is the length of the base of one of the triangle clumps along the length L. Figure 3.1 shows a top view of the total volume V. Assume that the height of V is defined by n layers of the cross section shown in Figure 3.1. The space between these layers shown by the side view in Figure 3.1 is also g_{defect}, and this is equivalent to the separation distance between clumps in the top view. The clump side length

q determines clump size. From Eqn 3.6, the expression for q is:

$$q = \frac{L}{n} - g_{defect} \tag{3.7}$$

Substituting $V = L^3$, $V_q = (nq)^3$ and Eqn 3.5 into Eqn 3.7, we find q as a function of the local packing fraction ϕ and bulk packing fraction.

$$q = \frac{g_{defect}\phi^{\frac{1}{3}}}{\phi^{\frac{1}{3}} - \phi_b^{\frac{1}{3}}} \tag{3.8}$$

We assume clumps are defined by three defects (as shown in Figure 3.1), which are weak points in the granular structure. Because three points are necessary to define a plane and a planar surface is the simplest boundary for a clump, we assume that three defects define a clump. Thus, we assume the base of the clump is an isosceles triangle and $A_{b,geo}$ is the cross-sectional area of the clump derived from the geometric constraints:

$$A_{b,geo} = \frac{1}{2}q^2 \tag{3.9}$$

To calculate the geometrically constrained clump volume, we must define the height of the clump. Following our development of the force constrained clump volume, we define the height of the geometrically constrained clump as $4a$. The volume occupied by the grains in a geometrically constrained clump is given by Eqn 3.10 and the number of grains in the clump is given by Eqn 3.11.

$$V_{b,geo} = 8\sqrt{2}R\phi A_{b,geo} \tag{3.10}$$

$$N_{grains} = \frac{V_{b,geo}}{V_g}$$

$$N_{grains} = \frac{3\sqrt{6}g_{defect}^2\phi^{\frac{5}{3}}}{2\pi R^2 \left(\phi^{\frac{1}{3}} - \phi_b^{\frac{1}{3}}\right)^2} \tag{3.11}$$

3.2 Clump Height's Impact on Geometric Clump Estimation

In standard crystalline packings, a single cube of volume will contain portions of grains in addition to whole grains (see Figure 3.2(a)). A real, physical clump of grains will only include whole grains. Imagine that the height of the clump defines the size of a box superimposed on the crystalline grain structure as illustrated in Figure 3.2. The clump will be defined by grains fully encompassed in this box, so removing the grains only partially inside the box will decrease the clump's true packing fraction ϕ_t from the nominal local packing fraction ϕ. Figure 3.2 shows, for FCC or HCP packing, how our definition of the clump height changes the true packing fraction from the nominal packing fraction, defined by the ratio of ϕ_t/ϕ. Figure 3.2 examines this ratio for the following heights: $2R$ (mono-layer clump), $2a$, q (uniform cubic clump), $3a$, and $4a$ (recall $a = 2\sqrt{2}R$ is the side length of an FCC packed cube).

In Figure 3.2, ϕ_t is calculated from the remaining grains and clump volume (between the cyan dashed lines) after partial grains are removed. The geometrically defined clump volume (Eqn 3.10) depends on the local packing fraction, bulk packing fraction, and grain radius. When ϕ_t/ϕ approaches 1, the clump volume given by the geometric model accurately predicts the clump volume calculated using the true

local packing fraction. We can see from Figure 3.2 that increasing the height h of the clump decreases the discrepancy between the nominal and true local packing fraction, causing ϕ_t/ϕ to approach 1. Our selection of $4a$ clump height yields a ratio ϕ_t/ϕ close to 1 (Figure 3.2(f)). The ratio $\phi_t/\phi = 0.96$ provides a correction factor between the nominal and true packing fraction for FCC packing with $h = 4a$, and applying it to our model gives the true geometric clump volume under these specific conditions. The true clump volume will be slightly less than predicted by our model. For the FCC or HCP packing ($\phi = 0.74$), $\phi_t = 0.710$. ϕ_t/ϕ will change with different local packings. Applying $\phi_t/\phi = 0.96$ as a correction factor for all $\phi < 0.74$ will lead to artificially larger clumps being predicted to detach on various bodies at looser local packing. Since we wish to be conservative in our prediction of largest detachable clump volume, we do not apply a correction factor to ϕ. Because our model treats the nominal packing fraction as equivalent to the true packing fraction, it leads to an underestimation of the detachable clump size.

(a) FCC packed cube

(b) $h = 2R$

(c) $h = 2a$

(d) $h = q$

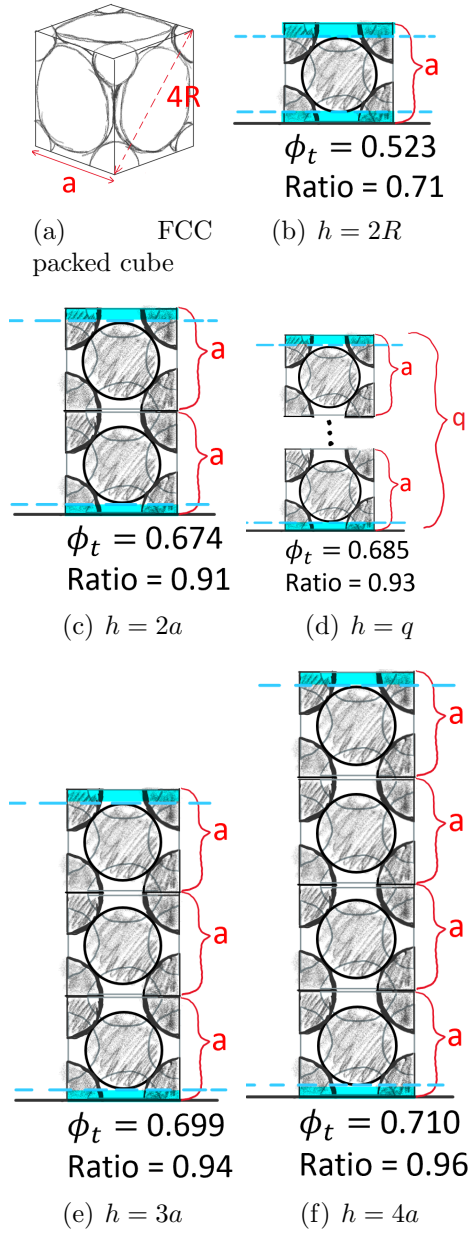(e) $h = 3a$

(f) $h = 4a$

Figure 3.2: The true local packing fraction ϕ_t (neglecting partial grains) and ratio ϕ_t/ϕ as a function of assumed clump height for an FCC-packed clump ($\phi = 0.74$), where $a = 2\sqrt{2}R$. The cyan regions show the sections of the clump removed when discarding layers of partial grains from the top and bottom of the clump when assuming some height h.

Chapter 4:   Clump Size Predictions

A clump must satisfy both the force constraint (Eqn 2.6) and the geometric constraint (Eqn 3.9). If the clump size dictated by the geometric constraint (Eqn 3.10) is smaller than the maximum clump size satisfying the force constraint (Eqn 2.7):

$$V_{b,geo} \leq V_{b,max} \tag{4.1}$$

then a clump, rather than an individual grain, will detach.

As mentioned previously, the local packing fraction is bounded by the bulk packing fraction and FCC packing:

$$\phi_b \quad \leq \quad \phi \quad \leq \quad \phi_{FCC} = 0.74 \tag{4.2}$$

When $\phi = \phi_b$, the local packing fraction of clumps matches the bulk packing fraction. As a result, no defects will exist, and the bulk powder will be uniformly packed. The maximum ϕ corresponds to FCC packing, with a value of 0.74. When $\phi = \phi_{FCC}$, clump volume is minimized because ϕ_{FCC} produces the largest allowable clump density.

4.1 Assumptions on Defect Length

We assume $g_{defect} \leq 2R$, since defects larger than the diameter of grains may become filled in situ. The total volume's porosity is composed of the empty space within clumps, driven by ϕ, and the sum of all defect volumes. Therefore, for a fixed local packing fraction ϕ, increasing g_{defect} will increase geometric clump side length (Eqn 3.8), thus increasing clump size. Smaller values of g_{defect} may be more realistic due to the size distribution of regolith in situ. In our model, when $g_{defect} > 1.2R$, the resulting detachable clumps (i.e., that satisfy Eqn 4.1) have a packing fraction greater than 0.74, which is not physical since the packing fraction must be less than the crystalline FCC packing. In the following results, the defect length is assumed to be R. Since we assume $g_{defect} = R$, increasing the local packing fraction decreases the geometric clump side length, which leads to a smaller clump size.

4.2 Maximum Detachable Clump on a Given Planetary Body

The maximum detachable clump size on a given planetary body is calculated by solving Eqn 4.1 for the local packing fraction that produces the equality constraint ($\phi_{max,size}$) and evaluating Eqn 3.10 at $\phi_{max,size}$.

$$\frac{1}{2}q^2 \leq \frac{8A_h R^2 C_{FCC} + \frac{32}{3}\pi R^4 \rho g}{A_h \phi_{max,size} C_{avg} + 64\sqrt{2}R^2 \phi_{max,size}\rho g} \tag{4.3}$$

We note that the centrifugal force has been dropped from Eqn 4.3 for simplicity. Substituting the definition for q from Eqn 3.8 into Eqn 4.3, we can re-write the

equation as a polynomial of $\phi_{max,size}$:

$$C_4\phi_{max,size}^{\frac{5}{3}} - C_1\phi_{max,size}^{\frac{2}{3}} + C_2\phi_{max,size}^{\frac{1}{3}} - C_3 \leq 0 \qquad (4.4)$$

$$C_1 = \frac{16A_hR^2C_{FCC} + \frac{64}{3}\pi R^4\rho g}{A_hC_{avg} + 64\sqrt{2}R^2\rho g}$$

$$C_2 = 2C_1\phi_b^{\frac{1}{3}}$$

$$C_3 = C_1\phi_b^{\frac{2}{3}}$$

$$C_4 = g_{defect}^2$$

Eqn 4.4 can be solved numerically for $\phi_{max,size}$ and then Eqn 3.10 can be used to calculate the maximum detachable clump size.

We will now present plots of clump size derived from the geometric ($V_{b,geo}$) and force ($V_{b,max}$) constraints as a function of local packing fraction, gravity and grain size. These plots show the range of clump sizes that can exist in situ and are easier to detach than individual grains.

4.3 Predicted Clumps on Bennu

Due to their low gravity, asteroids produce detachable clumps of relatively large grains. Figure 4.1 shows the clump size dictated by the force and geometric constraints for a variety of grain sizes, considering Bennu's surface gravity and spin rate (assuming a surface gravity of 8.60×10^{-5} m/s^2, 245 m mean radius, and 4.296 h rotation period [18]). We consider a bulk porosity of 55%, as Bennu's porosity is
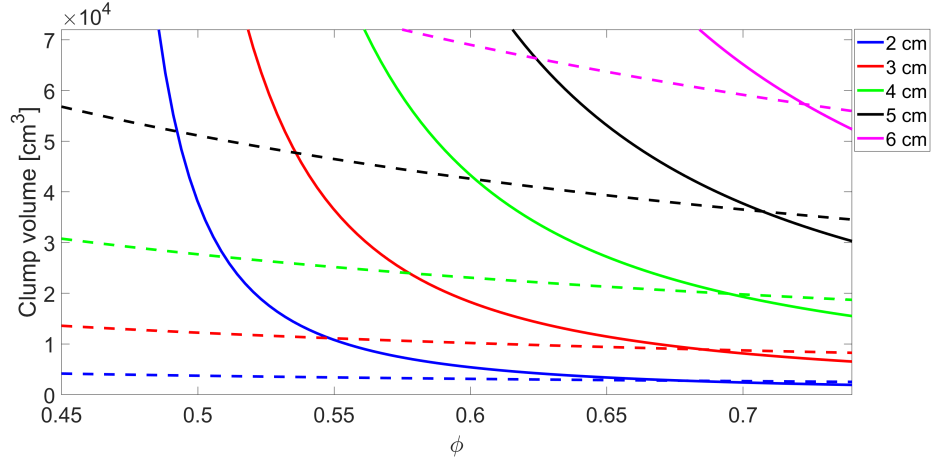
currently estimated to be at least 50% [18].

Figure 4.1: Clump volume as a function of grain size and local packing fraction on Bennu, assuming 0.45 bulk packing fraction. The dashed lines correspond to the maximum clump size from the force constraint and the solid lines represent the clump size from the geometric constraint. Clump sizes where the solid line is below the dashed line will be preferentially detached rather than individual grains.

Figure 4.1 shows predictions of the geometric and force constraint models and the resulting clumps that require less force to detach than individual grains. The intersection of a dashed line (force constraint) with the solid line (geometric constraint) of the same color indicates the maximum detachable clump size for that grain radius, occurring at $\phi_{max,size}$. The intersections occur at the lowest possible packing fraction for which clump detachment is possible. The largest detachable clump becomes more porous as grain size decreases. High packing fractions are difficult to achieve in nature, due to the polydispersity and asphericity of regolith in situ. Thus, the porous clumps (at packing fractions less than 0.74) are more likely to exist in nature. Recall that the geometric model used conservative conditions to predict larger clumps. Without these conditions, each solid line in Figure 4.1 would shift down due to smaller geometrically predicted clump sizes and cause its intersec-

tion point to shift towards the upper left of the figure, resulting in larger detachable clumps occurring at lower local packing fractions. Through our conservative geometric conditions, our approach under-predicts maximum detachable clump size. Figure 4.1 shows that centimeter-scale constituent grains produce decimeter-scale detachable clumps on Bennu. Similarly, Figure 4.2 demonstrates that millimeter-scale grains produce centimeter-sized clumps on Bennu.
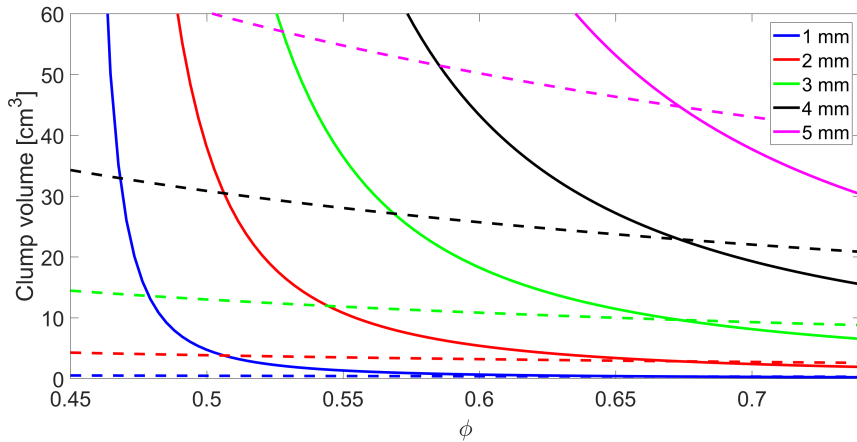

Figure 4.2: Clump volume as a function of grain size and local packing fraction on Bennu, assuming 0.45 bulk packing fraction. Grain radii on the millimeter scale are examined.

Figure 4.3 shows the number of grains per clump dictated by force and geometric constraints for a variety of grain sizes on Bennu. In Figure 4.3, the intersection of a dashed line with the solid line indicates the number of grains in the maximum clump size. Note that the solid line representing grains per clump from the geometric constraint is independent of grain size (because g_{defect} in Eqn 3.11 is a function of R). The grains per clump indicated by the dashed lines in Figure 4.3 are dependent upon the surface gravity on Bennu and the assumed grain size through Eqn 2.8. As grain radius decreases, the number of grains per clump increases from

approximately 45 to 57 grains. As grain size decreases, the number of grains per clump asymptotes to a value between 57 and 58 grains.
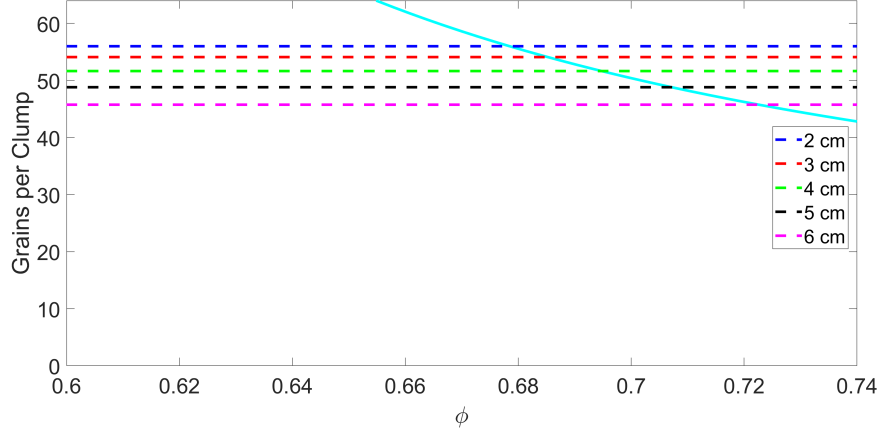

Figure 4.3: The number of grains per clump as a function of local packing fraction on Bennu, assuming 0.45 bulk packing fraction. The dashed lines correspond to the maximum number of grains per clump from the force constraint and the single solid line represents the number of grains per clump from the geometric constraint, which is independent of grain size (Eqn 3.11).

In our investigation, we assume that C_{avg}, the mean coordination number, is 4.5 for clumps [4] and the mean coordination number for grains is $C_{FCC} = 12$. Assuming 300 micron radius monodisperse grains on Bennu, Figure 4.4(a) shows how the volume of a clump varies with the assumed C_{avg}. The geometrically constrained clump volume (solid cyan curve in Figure 4.4(a)) is independent of C_{avg}. Decreasing C_{avg} from the nominal value of 4.5 significantly increases clump volume and decreases $\phi_{max,size}$. The cohesion force on a clump is proportional to C_{avg}, so reducing this force allows clumps to grow in size. Increasing C_{avg} gradually decreases clump size and significantly increases $\phi_{max,size}$. Detachment is impossible once $\phi_{max,size}$ exceeds 0.74 and becomes more unrealistic in nature as $\phi_{max,size}$ increases since higher values of ϕ require more idealized, near-crystalline packings. Figure 4.4(b) shows how the
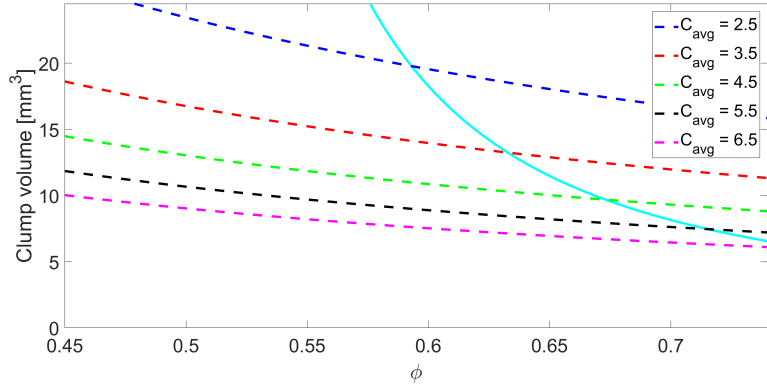
(a) $C_{FCC} = 12$
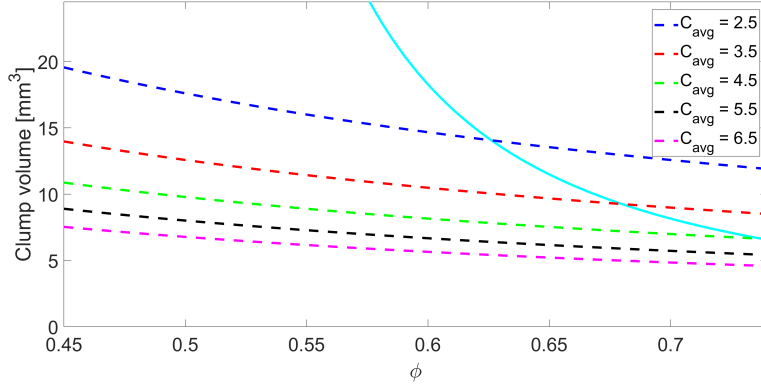
(b) $C_{FCC} = 9$

Figure 4.4: The volume of a clump on Bennu formed by 300 micron radius grains as a function of local packing fraction. Dashed lines correspond to the maximum clump volume from the force constraint, for a given C_{avg}, and the solid line represents the clump volume from the geometric constraint. Two values of C_{FCC} (number of contacts per grain) are considered.

results presented in Figure 4.4(a) change if we assume the mean coordination number for individual grains (C_{FCC}) is 9, reducing the cohesion on a single grain (Eqn 2.3). Reducing the cohesion on a grain makes the preferential detachment of a clump less likely in the force model. This is reflected in Figure 4.4(b) by a reduction in force-constrained clump size; all dashed lines shift downwards, causing maximum clump size to decrease and $\phi_{max,size}$ to increase. The solid line remains unchanged since geometric clump size is independent of cohesion force on a grain.

4.4 Predicted Clumps on Earth

Since Earth's gravity is 10^5 times stronger than Bennu's gravity, clumps of cm-scale grains will not exist on Earth, as discussed in Section 2.4, which is in agreement with our everyday interactions with granular materials on Earth. However, clumps of micron-scale grains are detachable on Earth (see Figure 4.5).
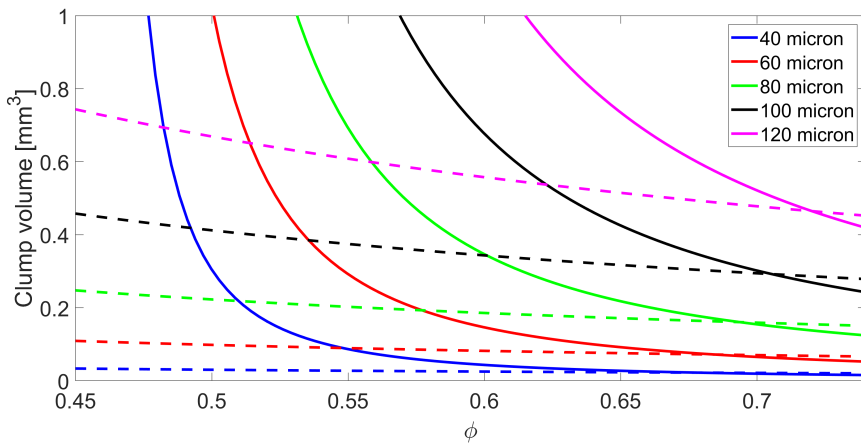

Figure 4.5: Clump volume as a function of grain size and local packing fraction on Earth, assuming 0.45 bulk packing fraction. The dashed lines correspond to the maximum clump size from the force constraint and the solid lines represent the clump size from the geometric constraint.

The clumping of micron-scale grains on Earth follows the same trends as clumping of centimeter-scale grains on Bennu. Additionally, the detachment of millimeter-scale clumps consisting of micron-scale constituent grains demonstrated by Figure 4.5 concurs with terrestrial studies of the size distribution of clumps formed in cohesive powder by micron scale grains on Earth [8]. The size distribution of clumps formed by cohesive powders on Earth has been experimentally measured for JSC-1A, 3 micron glass microbeads, and ordinary unbleached flour [8]. In Durda et al.'s [8] experiments, the granular material was sifted into a pile and then
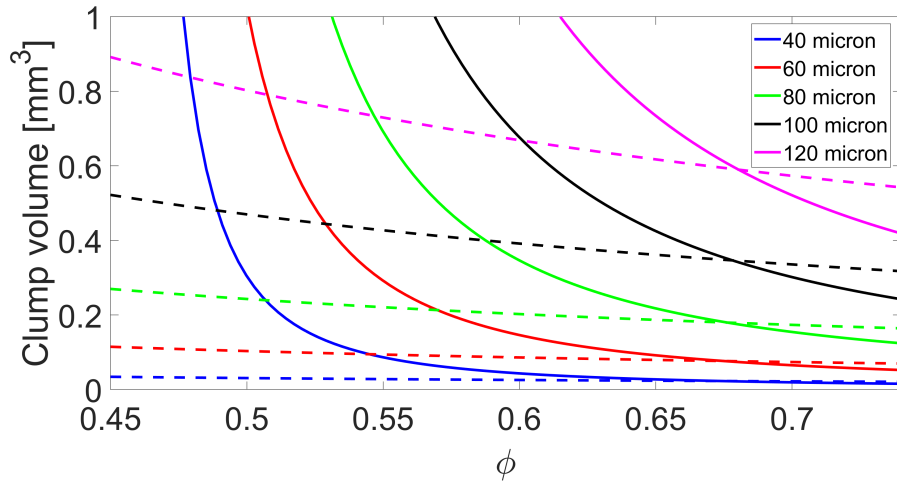
Figure 4.6: Clump volume as a function of grain size and local packing fraction on Earth, assuming 0.45 bulk packing fraction and flour density (0.507 g cm^{-3} for all-purpose white flour).

the pile was tilted until the slope failed. Clump sizes were measured after the slope failure (i.e., avalanche). The size distribution of clumps formed from flour indicates that most of these clumps are approximately 0.7 mm in diameter [8], with clumps up to 9 mm observed. Approximating these clumps as spherical, the volume of the average clump is 0.18 cubic millimeters. Figure 4.6 gives the maximum detachable clump volumes on Earth assuming the density of all-purpose white flour (0.507 g cm^{-3}) [19]. Figure 4.6 indicates that 0.18 cubic millimeter clumps can detach on Earth for a constituent grain radius of approximately 80 microns. Flour ranges in diameter from 75-570 microns [20, 21]. Thus, our results agree with the average clump size observed in Durda et al.'s [8] experiments, in spite of the differences between the method of clump detachment we envision in our model (where a clump is detached normally from a bed) and the experiment (where clumps travel downslope during avalanching). Additionally, note that the model results were obtained

using the Hamaker constant for lunar regolith. However, the Hamaker constant for baking flour ($\sim 6.5 \times 10^{-20}$) [22] is similar to that of lunar regolith ($\sim 5.14 \times 10^{-20}$). Our model does not predict clumps as large as 9 mm (as were observed much less frequently by Durda et al. [8]), which may be due to differences between the method of clump detachment between our model and the experiment or due to the conservative and simplifying assumptions made by our model (no atmosphere, spherical grains, uniformly sized grains).

The grain sizes studied in Figure 4.5 also correspond to medium to large carrier particle sizes commonly found in dry powder inhalers [9]. Thus, the formation of clumps (as predicted by this model) can inform dosing control as well as necessitate the shaking of inhalers (to break clumps) prior to use.

Chapter 5:   Conclusion

5.1   Overview

We have presented a model to predict the size of clumps that will be preferentially detached from the surface of body, rather than individual grains, as a function of grain size, local packing fraction, and the surface gravity. Regolith grains adhere to the surface of airless bodies due to a net downward force: the summation of cohesion and gravitational forces. Detachment of a grain occurs when this net downward force is overcome by some mechanism. Cohesion dominates the behavior of small particles and the formation of clumps is commonly observed on Earth. We show that, on asteroids, clumps of centimeter-scale and smaller grains are possible. Our predictions for clumps formed on Earth agree with extant experimental observations. These results are significant for understanding the motion and structural properties of regolith on the surface of planetary bodies as well as predicting clump sizes in a range of terrestrial powder handling applications (e.g., the pharmaceutical, coal mining, and food production industries).

5.2 Implications: Small Asteroids

The force constraint determines the clump size that is easier to detach than an individual, constituent grain. The geometric constraint predicts the clump size present in situ given the bulk packing fraction. Given these two constraints, we can predict the clump sizes that are easier to detach in situ than their constituent grains, for a range of grain sizes, packing fractions, and surface gravities.

On small asteroids like Bennu, we predict that centimeter-scale and smaller grains are capable of producing detachable clumps. As grain size decreases, the largest detachable clump becomes more porous. The largest clump that can be detached is a function of both the grain size and the local packing fraction. For a given grain size, as the packing fraction increases, the clump size decreases. For a given grain size, the smallest clump will occur at a local packing fraction corresponding to FCC packing. However, it is unlikely that high local packing fractions will occur in situ due to the asphericity of regolith grains.

The OSIRIS-REx mission has observed particles ranging from centimeters to meters in size on the asteroid Bennu [23]. Our model predicts that clumps up to 40cm in size can be formed from cm-scale constituent grains on Bennu (see 4.1). Additionally, we predict that centimeter-scale clumps could be formed from millimeter-scale constituent grains. These predictions influence the interpretation of visual observations of the surface of small, rocky asteroids, challenging the assumption that an observed 'rock' is coherent, and not, in fact, a clump, as has been proposed by Durda et al. [8]. Further, our model predicts the preferential detachment of

37

centimeter-scale clumps (rather than millimeter-scale constituent grains), which also concurs with observations of "airfall" from active regions on comet 67P/Churyumov-Gerasimenko (CG) [24] and the ejection of dm-scale aggregates [25].

We have assumed that the force acting to detach a grain or clump from the surface is collinear with gravity and the net cohesive force. Depending on the grain detachment mechanism, this assumption may not be accurate (e.g., for particle entrainment in aeolian flows on Mars, and on asteroids, where the local gravity may not be normal to the surface). This analysis could be re-visited considering the appropriate components of the detaching and restraining forces. The analysis would not change significantly as long as there is some component of the detaching force that is normal to the surface. If the detaching force only has a tangential component, then a different approach should be taken. Nonetheless, the analysis presented here provides a first order quantitative prediction of preferential clump detachment and the sizes of detachable clumps.

5.3   Implications: Martian Aeolian Processes

On Mars, the grain size in sand dunes was predicted to be 500 microns in diameter from thermal inertia data [12] and observations conducted by the Mars Exploration Rover of the Eagle crater floor reveal basaltic grains down to even 50 to 125 micron in size [26]. From Figure 2.3, we can see that for Martian gravity, grains below 500 micron in size can form clumps consisting of multiple grains that are easier to detach from the surface. Thus, the size distribution of particles in

Martian sand dunes derived from thermal observations could include clumps.

Prior experimental work has shown that airborne particles may clump together due to electrostatic charging [27] and that the formation of surficial regolith clumps may influence the erosion rate of Martian surface features [28]. Our work quantifies the cohesive and gravitational forces acting on particles, and predicts the size of agglomerates that are easier to detach from the surface. The lofting of aggregates rather than individual grains due to aeolian stresses agrees with experimental observations by Marshall et al. [5].

5.4   Realistic Regolith Considerations

Planetary regolith grains are not spherical but highly angular [29]. The angularity of real regolith grains may produce local packing fractions that are larger or smaller than the spherical limit, depending on the history of the surface (e.g., compaction or expansion due to impact-induced vibration). For the force model, variation in the local packing fraction will influence the gravitational force. Accounting for aspherical grains in the geometric model is complex since the shape of the grains influences the size and frequency of defects between clumps, which are the driving factors for clump size. With increasingly large grain sizes, interparticle cohesion would be driven more by the local curvature radii at contact points rather than grain size directly [16].

Additionally, planetary regolith is polydisperse. A polydisperse mixture would influence the force model by increasing the local packing fraction, as smaller grains

would fill in void spaces within clumps. This would lead to heavier clumps, which would result in smaller maximum clump sizes. Again, extension of the geometric model to the polydisperse mixture is more complicated than the modification of the force model. The total volume of the defects does not change for given bulk and local packing fractions, but the physical constraint on the length of the defects is removed since there are multiple grain sizes.

5.5 Cohesion & Terrestrial Results

Detaching grains from the surface reduces their mean coordination number from 12 to 9. For monodisperse spherical grains, Figure 4.4(b) shows that assuming $C_{FCC} = 9$ leads to smaller clumps and tighter local packing. However, experimental work on terrestrial clumping using flour powder [8] observed that grains between 75-570 micron diameter produce mm scale clumps on Earth, also predicted by our monodisperse terrestrial model for grain mean coordination number of 12 (4.5). Flour used in these experiments features polydisperse and aspherical grains that can increase the mean coordination number for a grain from 9 towards 12, causing a grain to experience more cohesion. Thus, while we have assumed spherical, monodisperse particles with 12 contacts ($C_{FCC} = 12$), our predictions still agree with existing experimental observations of more realistic powders.

Despite the simplified grain size and shape model used, the model presented here produces clump sizes that are in agreement with terrestrial experimental results with polydisperse, apsherical powders [8]. Thus, this model provides a first order

estimate of clump sizes expected to be present and possible to detach on a variety of planetary bodies, including Earth.

5.6   Future Work

The next step for our research would be experimental validation of our predictions for clump size using mono-disperse, spherical grains. These experiments would seek to validate the terrestrial results presented in Section 4.4. Experiments from Durda et al. [8] use highly angular, polydisperse flour grains and an avalanching technique to generate clumps. Our future experiments would likely use spherical beads, such as the polystyrene microspheres in Hartzell et al. [3], as regolith simulant and study the preferential detachment of clumps through perpendicular force, rather than lateral as presented by avalanching. These experiments would be carried out under vacuum, preventing moisture from artificially increasing cohesion.

Since both regolith grains and boulders on small bodies range in size, the effect of polydisperse grain size on clump size distribution is of great interest. Our model can be extended to study the clump size distribution for a given local packing fraction, gravity, and set of grain sizes using Monte-Carlo Simulations. The results of these methods would give us a better estimate for average clump size on a given body.

Bibliography

[1] D. J. Scheeres, C. M. Hartzell, P. Sánchez, and M. Swift, "Scaling forces to asteroid surfaces: The role of cohesion," *Icarus*, vol. 210, no. 2, pp. 968–984, 2010.

[2] C. M. Hartzell and D. J. Scheeres, "The role of cohesive forces in particle launching on the moon and asteroids," *Planetary and Space Science*, vol. 59, no. 14, pp. 1758–1768, 2011.

[3] C. Hartzell, X. Wang, D. Scheeres, and M. Horányi, "Experimental demonstration of the role of cohesion in electrostatic dust lofting," *Geophysical Research Letters*, vol. 40, no. 6, pp. 1038–1042, 2013.

[4] P. Sánchez and D. J. Scheeres, "The strength of regolith and rubble pile asteroids," *Meteoritics & Planetary Science*, vol. 49, no. 5, pp. 788–811, 2014.

[5] J. Marshall, D. Richard, and S. Davis, "Electrical stress and strain in lunar regolith simulants," *Planetary and Space Science*, vol. 59, pp. 1744–1748, 2011.

[6] P. Helfenstein and M. Shepard, "Submillimeter-scale topography of the lunar regolith," *Icarus*, vol. 141, pp. 107–131, 1999.

[7] D. Durda, S. Roark, D. Scheeres, P. Sanchez, G. Devaud, P. Kaptchen, and R. Dissly, "Experimental approach and apparatus for laboratory investigation of asteroid regolith properties," in *Lunar and Planetary Science Conference*, vol. 44, p. 2287, 2013.

[8] D. Durda, P. Sanchez, A. Fischer, G. Devaud, D. Scheeres, S. Roark, P. Kaptchen, and R. Dissly, "The size distribution of 'boulders' formed during slope failure in piles of self-cohesive powders: Application to the morphology of regoliths on small asteroids," in *Lunar and Planetary Science Conference*, vol. 45, p. 2015, 2014.

[9] M. J. Donovan, S. H. Kim, V. Raman, and H. D. Smyth, "Dry powder inhaler device influence on carrier particle performance," *Journal of pharmaceutical sciences*, vol. 101, no. 3, pp. 1097–1107, 2012.

[10] K. L. Cashdollar, "Coal dust explosibility," *Journal of loss prevention in the process industries*, vol. 9, no. 1, pp. 65–76, 1996.

[11] N. Kagi, S. Fujii, Y. Horiba, N. Namiki, Y. Ohtani, H. Emi, H. Tamura, and Y. S. Kim, "Indoor air quality for chemical and ultrafine particle contaminants from printers," *Building and Environment*, vol. 42, no. 5, pp. 1949–1954, 2007.

[12] K. S. Edgett and P. R. Christensen, "The particle size of martian aeolian dunes," *Journal of Geophysical Research: Planets*, vol. 96, no. E5, pp. 22765–22776, 1991.

[13] R. Greeley, N. Lancaster, S. Lee, and P. Thomas, "Martian aeolian processes, sediments, and features," *Mars*, pp. 730–766, 1992.

[14] I. J. Smalley, "Cohesion of soil particles and the intrinsic resistance of simple soil systems to wind erosion," *Journal of Soil Science*, vol. 21, no. 1, pp. 154–161, 1970.

[15] A. Patel and C. Hartzell, "Cohesive regolith clump size prediction on airless bodies," in *Lunar and Planetary Science Conference*, vol. 50, 2019.

[16] L. Starukhina, "Characteristics of the contact between regolith particles: their influence on the physical properties of regoliths," *Solar System Research*, vol. 34, p. 295, 2000.

[17] T. C. Hales, "An overview of the kepler conjecture," *arXiv preprint math/9811071*, 1998.

[18] D. Lauretta, D. DellaGiustina, C. Bennett, D. Golish, K. Becker, S. Balram-Knutson, O. Barnouin, T. Becker, W. Bottke, W. Boynton, *et al.*, "The unexpected surface of asteroid (101955) bennu," *Nature*, vol. 568, no. 7750, p. 55, 2019.

[19] S. Gebhardt, L. Lemar, P. Pehrsson, J. Exler, D. Haytowitz, K. Patterson, *et al.*, "Usda national nutrient database for standard reference, release 22. usda national nutrient database for standard reference," 2007.

[20] S. D. Sakhare, A. A. Inamdar, C. Soumya, D. Indrani, and G. V. Rao, "Effect of flour particle size on microstructural, rheological and physico-sensory characteristics of bread and south indian parotta," *Journal of food science and technology*, vol. 51, no. 12, pp. 4108–4113, 2014.

[21] A. Patwa, B. Malcolm, J. Wilson, and K. R. Ambrose, "Particle size analysis of two distinct classes of wheat flour by sieving," *Transactions of the ASABE*, vol. 57, no. 1, pp. 151–159, 2014.

[22] K. Siliveru, *Cohesive Properties of Wheat Flour and Their Effect on the Size-Based Separation Process*. PhD thesis, Kansas State University, 2016.

[23] K. Walsh, E. Jawin, R.-L. Ballouz, *et al.*, "Craters, boulders and regolith of (101955) bennu indicative of an old and dynamic surface," *Nature Geophysics*, vol. 12, no. 4, pp. 242–246, 2019.

[24] N. Thomas, B. Davidsson, M. R. El-Maarry, S. Fornasier, L. Giacomini, A. Gracia-Berná, S. Hviid, W.-H. Ip, L. Jorda, H. Keller, *et al.*, "Redistribution of particles across the nucleus of comet 67p/churyumov-gerasimenko," *Astronomy & Astrophysics*, vol. 583, p. A17, 2015.

[25] J. Agarwal, M. A'Hearn, J.-B. Vincent, *et al.*, "Acceleration of individual, decimetre-sized aggregates in the lower coma of comet 67P/Churyumov-Gerasimenko," *Monthly Notices of the Royal Astronomical Society*, vol. 462, pp. S78–S88, 2016.

[26] R. Sullivan, D. Banfield, J. F. Bell III, W. Calvin, D. Fike, M. Golombek, R. Greeley, J. Grotzinger, K. Herkenhoff, D. Jerolmack, *et al.*, "Aeolian processes at the mars exploration rover meridiani planum landing site," *Nature*, vol. 436, no. 7047, p. 58, 2005.

[27] R. Greeley, "Silt-clay aggregates on mars," *Journal of Geophysical Research: Solid Earth*, vol. 84, no. B11, pp. 6248–6254, 1979.

[28] R. Greeley, R. N. Leach, S. H. Williams, B. R. White, J. B. Pollack, D. H. Krinsley, and J. R. Marshall, "Rate of wind abrasion on mars," *Journal of Geophysical Research: Solid Earth*, vol. 87, no. B12, pp. 10009–10024, 1982.

[29] A. Tsuchiyama, M. Uesugi, T. Matsushima, T. Michikami, T. Kadono, T. Nakamura, K. Uesugi, T. Nakano, S. A. Sandford, R. Noguchi, *et al.*, "Three-dimensional structure of hayabusa samples: origin and evolution of itokawa regolith," *Science*, vol. 333, no. 6046, pp. 1125–1128, 2011.